

STUDY OF THE LAMINAR JET IMPINGING ON A FLAT SURFACE

Fábio Yukio Kurokawa, kurokawa@ita.br
Edson Luiz Zapparoli, zapparoli@ita.br
Cláudia Regina de Andrade, claudia@ita.br

Instituto Tecnológico de Aeronáutica
Grupo de Simulação de Escoamentos e Transferência de Calor
Praça Mar Eduardo Gomes, 50 – Vila das Acácias
CEP 12 228 – 900, São José dos Campos – SP

Abstract. Impingement jet heat transfer has been well established as an effective technique for heating, cooling or drying a target surface and is employed in many important applications. At this work, a numerical study applying the control volume numerical scheme is carried out to analyze the flow and heat transfer of a impingement jet normal to a flat surface. The convective terms were discretized using different interpolation schemas to study the influence on local Nusselt number in the impingement wall. The discretized equations were solved by a segregated formulation using the SIMPLE approach for the pressure-velocity coupling. The problem considered is of a circular jet laminar air flow (Prandtl number equal to 0.71) with Reynolds number ranging from 100 to 1000 with constant nozzle-to-surface spacing of the $H/D = 2$. An unstructured mesh with quadrilateral elements were employed to obtain the numerical solution. The influence of radial domain extension in the results is also analyzed for $r/D = 2.5, 5, 7.5$ and 10. To validate the results, a comparison with available literature data is performed. The results shows that the interpolation schema and the radial domain extension don't affect the Nusselt number in the studied parameters range.

Keywords: Impingement jet, finite volume method, CFD, interpolation schemas, laminar flow.

1. INTRODUCTION

Jet impingement heating and cooling is used in many engineering and industrial applications, such as materials processing, manufacturing, drying and cooling of computers and electronic equipment, Behnia et al., (1998). There are numerous studies, mostly experimental, on the flow characteristics and heat transfer associated with jet impingement on surfaces, Baughn and Shimizu, (1989). The advantages of impingement heat transfer process are direct, localized heating or cooling, and increased heat fluxes.

There are a number of parameters which can affect the heat transfer rate in a jet impingement configuration, Behnia et al., (1997). For the design and optimization of jet impingement cooling or heating systems, it is essential that the effect of these parameters of importance be characterized. These parameters are often quite different (and sometimes unknown) for different experimental studies of impingement heat transfer making it difficult to compare or generalize experimental results, Baughn et al. (1991).

Due to the difficulties in performing and comparing experiments, a numerical simulation of the problem would have been an ideal candidate for quantifying the effect of the parameters of interest, Behnia et al., (1997). Laminar and turbulent impinging jets have complex features due to entrainment, stagnation, and high streamline curvature. These features prove to be incompatible with most existing turbulence models, which are essentially developed and tested for flows parallel to a wall.

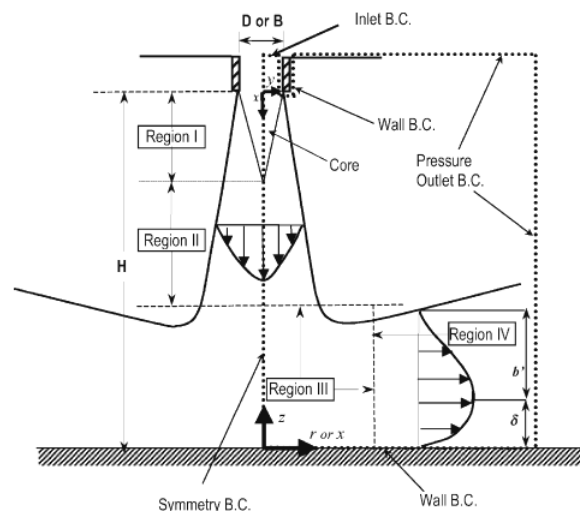


Figure 1. Characterization of impinging jets for single round nozzle jet, Coussirat et al. (2005).

In the impingement region, the mean flow is perpendicular (or nearly perpendicular) to the surface, Fig. 1. It then turns and follows the surface in a wall jet. In the stagnation region, the flow is nearly irrotational and there is a large total strain along the stagnation streamline. Away from the core of the jet there is substantial curvature of the streamlines. Adjacent to the wall, there are thin stagnation points and wall jet boundary layers on the target plate.

Chattopadhyay (2004) presents numerical results for an annular jet in the laminar regime. The heat transfer from the annular jet is compared with the circular jet at the same value of Reynolds number (Re) while keeping momentum efflux at the nozzle exit at the same level. This author was found that heat transfer from the annular jet was about 20% less compared to the circular jet.

An application of the impingement jet is in the removal and/or prevention of ice on aircraft component, de-icing and anti-icing systems, respectively, Wright (2004), because the atmospheric icing presents a major hazard to aircraft operating. This is also the cause of major concerns for the certification authorities as well as the aircraft manufacturers, Saeed et al. (2000).

A critical aspect in the design of an anti-icing system is the prediction of the heat transfer of the impinging jets from the piccolo tube, Brown et al. (2002).

This work presents numerical simulations of the laminar impingement jet on a flat plate with constant nozzle-to-surface spacing of the $H/D = 2$. The problem considered is air flow (Prandtl number equal to 0.71) of an axisymmetric jet impinging onto a heated wall with Reynolds number ranging from 100 to 1000. The influence of interpolation schema and radial domain extension on local Nusselt number was analyzed.

2. DESCRIPTION OF PROBLEM

The airflow problem was assumed to be laminar, incompressible, neglecting the effects of gravity and viscous dissipation. Air is modeled as Newtonian fluid with constant physical properties. Based on these assumptions, numerical simulations of the flow and thermal field in the laminar unconfined jet impinging on the flat plate were performed.

The schematic representation of the axis-symmetrical impingement jet configuration as well as imposed boundary conditions is showed in Fig. 2.

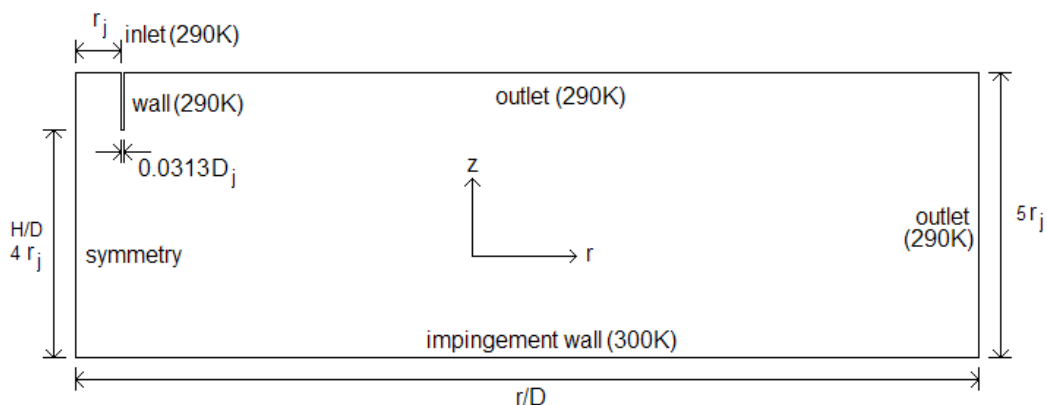


Figure 2. Schematic of the geometry used in the simulations.

The Reynolds number is defined according to the characteristic length D_j (jet diameter) and velocity scale V_j (uniform jet velocity):

$$Re = \frac{\rho V_j D_j}{\mu} \quad (1)$$

where ρ - fluid density and μ - fluid dynamic viscosity.

In Fig. 2, the surface distance (H) was maintained constant and equal to $2D_j$.

3. MATHEMATICAL MODELING

The steady-state Navier-Stokes (N-S) equations for an incompressible laminar airflow with constant properties fluid are presented in the two-dimensional cylindrical coordinate system (r, z). It is assumed that the viscous heating and gravity effects are negligible.

Continuity equation:

$$\frac{1}{r} \left(\frac{\partial(rv_r)}{\partial r} \right) + \frac{\partial v_z}{\partial z} = 0 \quad (2)$$

Momentum equation in radial direction:

$$v_r \frac{\partial v_r}{\partial r} + v_z \frac{\partial v_r}{\partial z} = -\frac{\partial p}{\partial r} + \frac{1}{Re} \left(\nabla^2 v_r - \frac{v_r^2}{r} \right) \quad (3)$$

Momentum equation in axial direction:

$$v_r \frac{\partial v_z}{\partial r} + v_z \frac{\partial v_z}{\partial z} = -\frac{\partial p}{\partial z} + \frac{1}{Re} (\nabla^2 v_z) \quad (4)$$

Energy equation:

$$v_r \frac{\partial T}{\partial r} + v_z \frac{\partial T}{\partial z} = \frac{1}{Pr \cdot Re} (\nabla^2 T) \quad (5)$$

with $Pr = \frac{\mu C_p}{k}$ - Prandtl number, C_p - constant pressure specific heat; k - fluid thermal conductivity;

The boundary conditions represented in Fig. 2 are:

a) Inlet: $v_z = -V_j, v_r = 0, T = T_j, \frac{\partial P}{\partial z} = 0$;

b) Outlet: $p = 0$, if $\begin{cases} v_n \leq 0, \frac{\partial T}{\partial n} = 0, \frac{\partial v_z}{\partial n} = 0, \frac{\partial v_r}{\partial n} = 0 \\ v_n > 0, T = T_j \end{cases}$ where n is the surface normal vector;

c) Wall: $v_z = 0, v_r = 0, T = T_w$;

d) Symmetry: $v_r = 0, \frac{\partial v_z}{\partial r} = 0, \frac{\partial T}{\partial r} = 0, \frac{\partial P}{\partial r} = 0$.

where T_j and T_w are the jet and wall temperatures, respectively.

4. COMPUTATIONAL APPROACH

The numerical simulations were carried out using the commercial CFD software, FLUENT™ (2006) version 6.2.16. The governing equations were solved by a finite volume method (Fletcher, 1998), which involves integrating the equations about each control volume. The convective terms in all equations were discretized using five different interpolation schemes. The discretized equations were solved by a segregated formulation, using the SIMPLE approach for pressure-velocity coupling.

The impingement jet problem is solved employing a procedure that comprises three steps: pre-processor, solver and post-processor:

- pre-processor: drawing of geometric domain (space occupied by the fluid flow); grid generation (domain subdivision in small finite elements or finite volumes) and physics, mathematical and numerical setups (mathematical model, fluid properties, numerical approach, boundaries and initial conditions);
- solver: computational solution of the algebraic equations systems obtained after the governing equation discretization (usually employing iterative algorithms);
- post-processor: quantitative and qualitative (visualization) analysis of the obtained results.

The simulations were performed using a mesh with quadrilateral elements, running in a Workstation AMD 64 (OS Linux).

5. RESULTS

To validate the numerical tool, a comparison with experimental data provided by Chattopadhyay (2004) for the local Nusselt number is performed. An analysis of grid independence was performed using four different meshes. Table 1 summarizes the number of elements for each mesh at different domain radial extension to jet diameter ratio (r/D).

Table 1. Number of cells for each mesh.

r/D	Mesh 1 (cells)	Mesh 2 (cells)	Mesh 3 (cells)	Mesh 4 (cells)
2.5	10,000	55,000	157,000	430,000
5	24,000	52,000	141,000	286,000
7.5	12,000	37,000	140,000	336,000
10	16,000	78,000	137,000	320,000

Figure 3 illustrates the computational domain ($r/D = 10$) with the finest grid (320,000 cells) and a zoom closed to jet exit and neighborhood of the symmetry axis. Note that, it is required a refined mesh to capture the jet shear and boundary layers. Other phenomena, as the strong streamlines curvature when the jet turns from the axial to the radial direction, also need a dense grid.

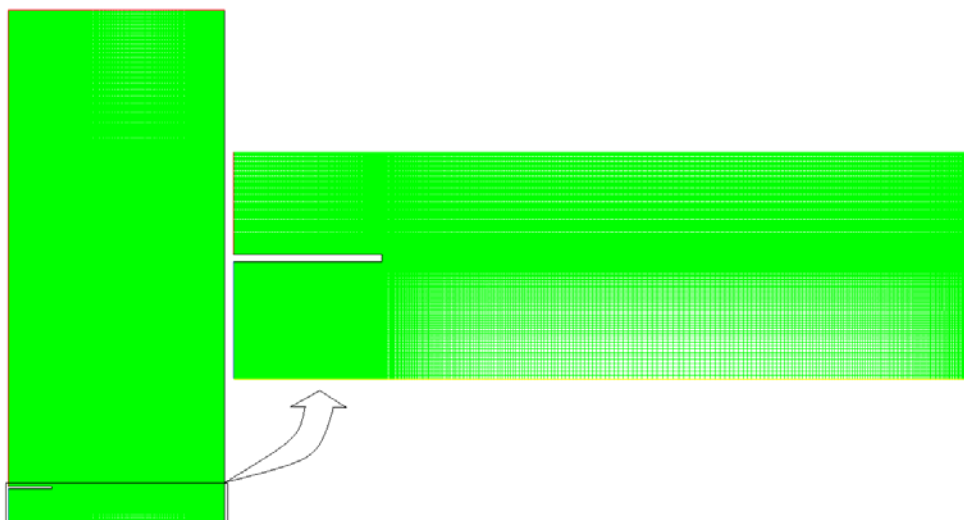


Figure 3. Example of mesh utilized in the simulations.

Table 2 present the improvements obtained with mesh refinement for mass flow rate and total heat transfer rate balances as a function of r/D parameter. As the mesh is denser, the mass flow and heat transfer balances results are better. This is an important verification during the numerical solution procedure.

Table 2 – Comparison of results obtained with mesh refinement.

r/D	mesh	cells	mass flow rate	total heat transfer rate
2.5	1	11,000	5.43E-8	-4.04E-4
	4	430,000	2.65E-9	-8.32E-5
5	1	24,000	3.43E-8	-2.46E-3
	4	280,000	7.43E-10	-1.34E-4
7.5	1	12,000	2.99E-8	-1.79E-3
	4	336,000	6.88E-10	-3.52E-4
10	1	16,000	6.09E-9	-4.73E-3
	4	320,000	1.38E-9	-2.39E-4

Figure 4 to Figure 7 present the mesh refinement study based on the local Nusselt number results at $r/D = 2.5, 5,$

7.5 and 10 with Reynolds number equal to 1000. The experimental data for $r/D = 5$ are also presented for comparison. The local Nusselt number is calculated as:

$$Nu = \frac{hD_j}{k} \quad \text{where} \quad h = \frac{q_w}{(T_w - T_f)} \quad (6)$$

where k - fluid thermal conductivity and q_w - heat flux at the impingement wall.

The grid independent solution was attained, as observed in Fig. 4 to Fig. 7. For r/D range studied, the results show larger discrepancy in the stagnation region, near the Nusselt number pick, and a good agreement outside stagnation region. In the stagnation region, the flow presents greater properties gradients and streamlines curvature.

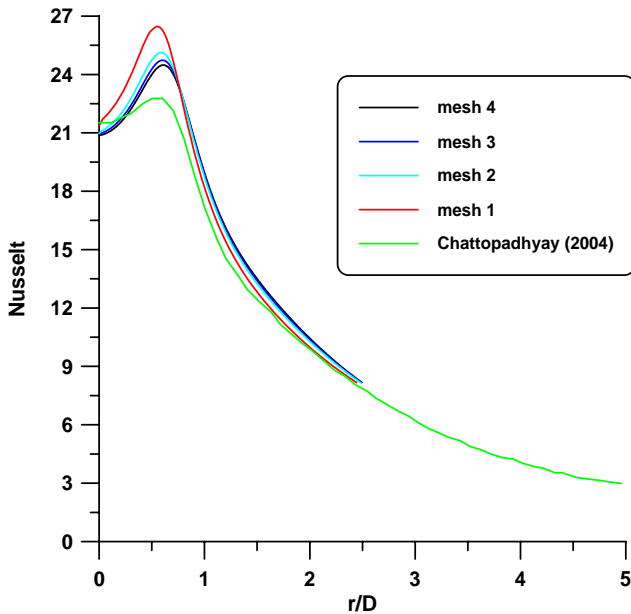


Figure 4. Local Nusselt number for different meshes and $r/D = 2.5$.

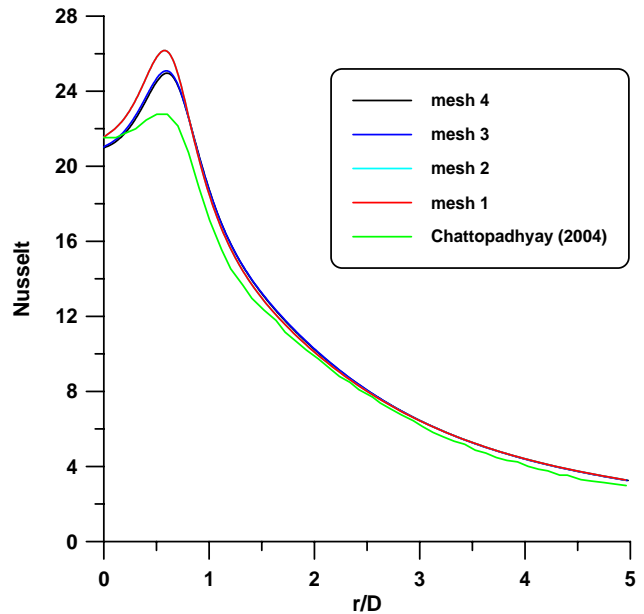


Figure 5. Local Nusselt number for different meshes and $r/D = 5$.

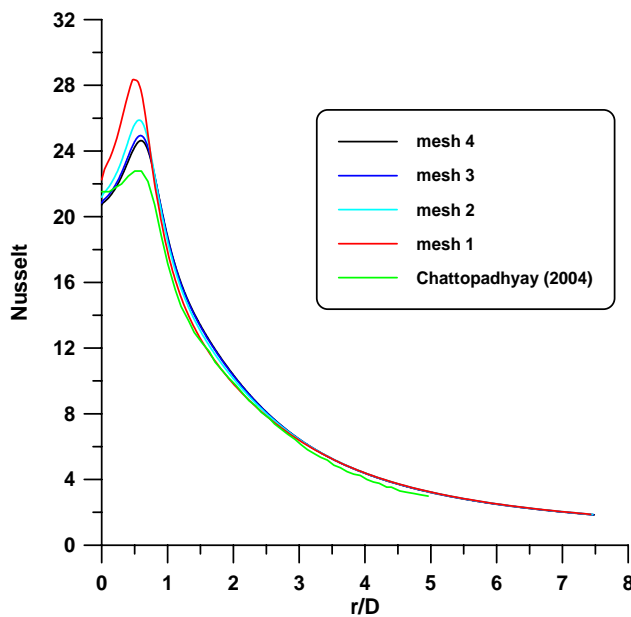


Figure 6. Local Nusselt number for different meshes and $r/D = 7.5$.

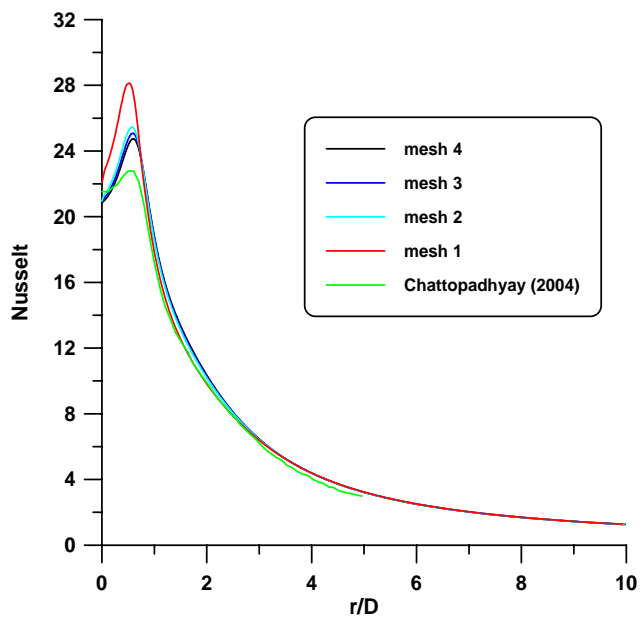


Figure 7. Local Nusselt number for different meshes and $r/D = 10$.

The analysis of the convective term discretization schemes effect has been done for Reynolds number equal to 1000. Five discretization schemes have been considered, Upwind (First and Second order), Power Law, QUICK and Third-order. Figure 8 to Figure 10 present the discretization effect for the coarsest (mesh 1) and finest (mesh 4) mesh, for $r/D = 5, 7.5$ and 10, respectively.

The first-order scheme introduces a dissipative error that is stabilizing and helps the solver achieve robust convergence. The second-order scheme attempts to minimize both dispersive and dissipative errors to give a result that is always more accurate than the first-order one. The power law scheme is a more accurate approximation, interpolates the face value of a variable using the exact solution to a one-dimensional convection-diffusion equation. QUICK type schemes are based on a weighted average of second-order upwind and central interpolations of the variable. The Third-order convection was conceived from the original MUSCL (Monotone Upstream Centered Schemes for Conservation Laws) by blending a central differencing scheme and second-order upwind scheme.

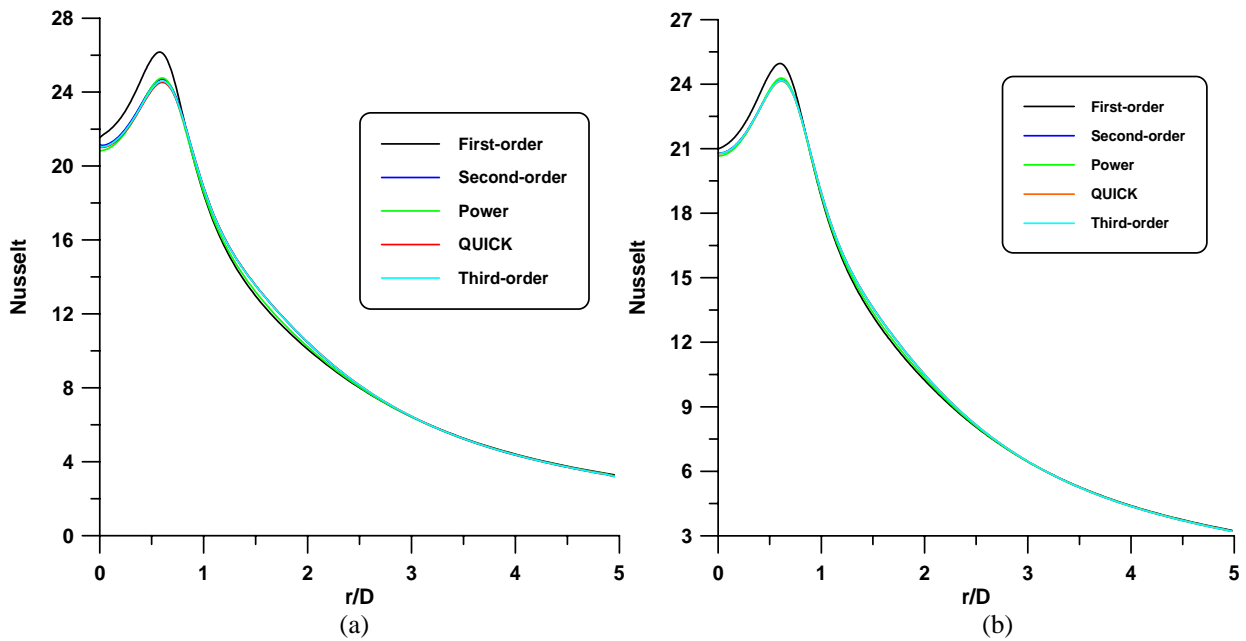


Figure 8. Comparison of results for different discretization schemes with $r/D = 5$ for (a) mesh 1 and (b) mesh 4.

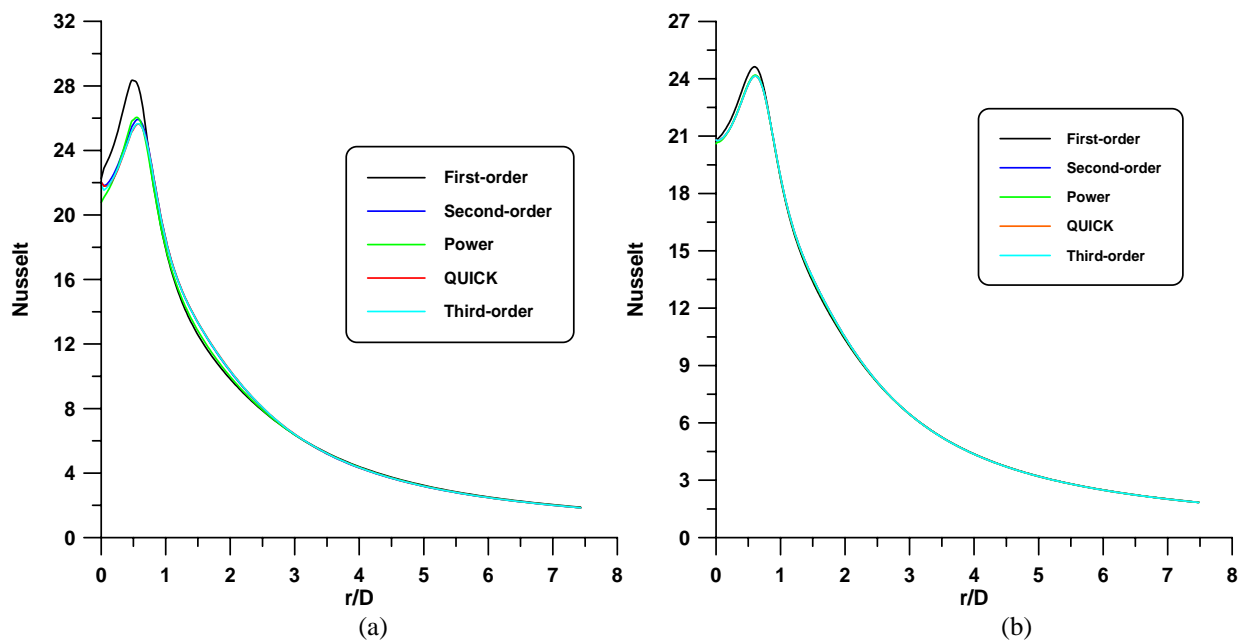


Figure 9. Comparison of results for different discretization schemes with $r/D = 7.5$ for (a) mesh 1 and (b) mesh 4.

The effects of convective terms discretization are greater in the coarsest grid (mesh 1). These effects are stronger in the stagnation region, where occur largest properties gradients and the grid faces cells aren't aligned with velocity flow vector. As expected, the first-order discretization presents the greater discrepancy in the stagnation region.

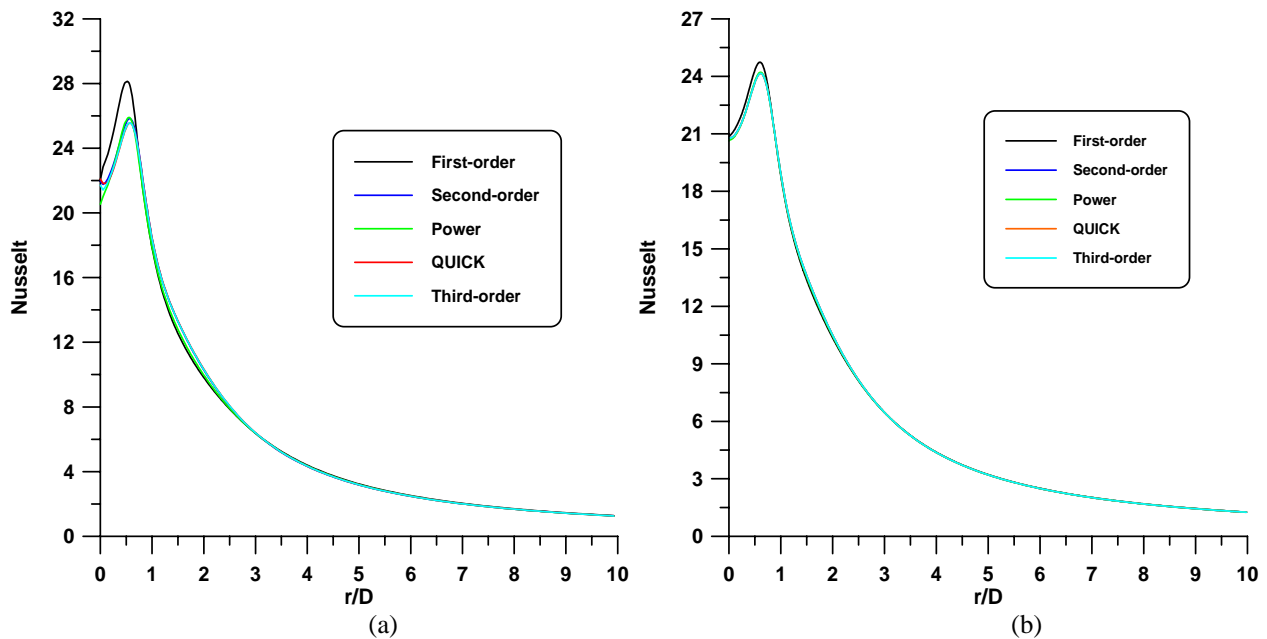


Figure 10. Comparison of results for different discretization schemes with $r/D = 10$ for (a) mesh 1 and (b) mesh 4.

Figure 11 to Figure 16 present the effects of Reynolds number and domain radial extension on local Nusselt number in the impingement surface. The Reynolds number ranging from 100 to 1000 and domain radial extension ranging from 2.5 to 10, using the finest mesh (mesh 4) were studied.

The domain radial extension doesn't affect any results because the flow and heat transfer are parabolic in the radial direction, that is, the effects propagate only in the positive radial direction. Therefore, the results for lower r/D values can be obtained from the larger r/D domain extension.

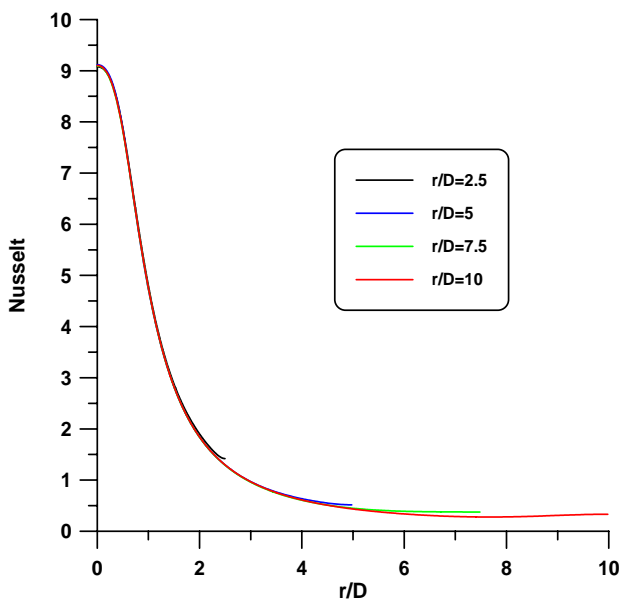


Figure 11. Local Nusselt number in the impingement surface for $Re=100$.

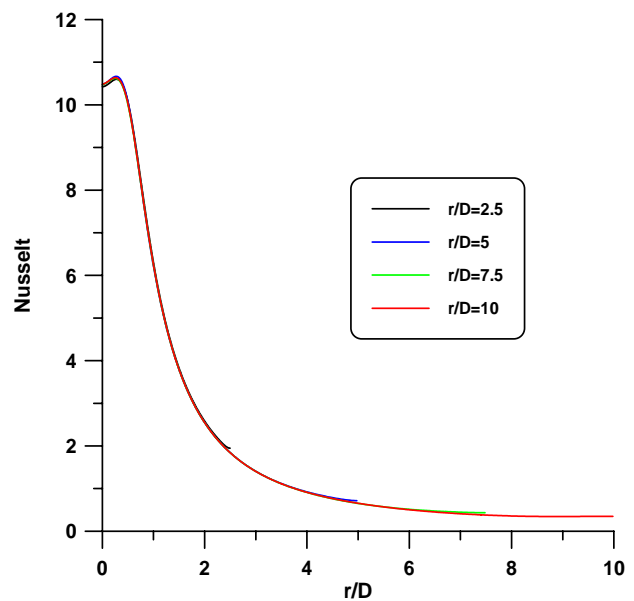


Figure 12. Local Nusselt number in the impingement surface for $Re=150$.

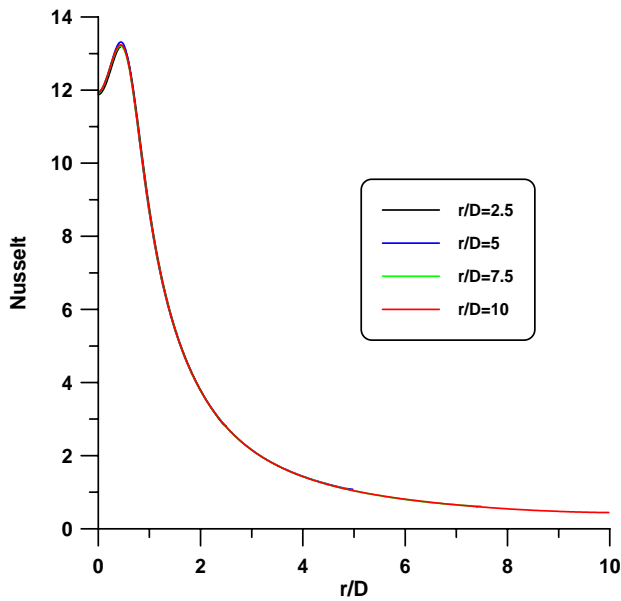


Figure 13. Local Nusselt number in the impingement surface for Re=250.

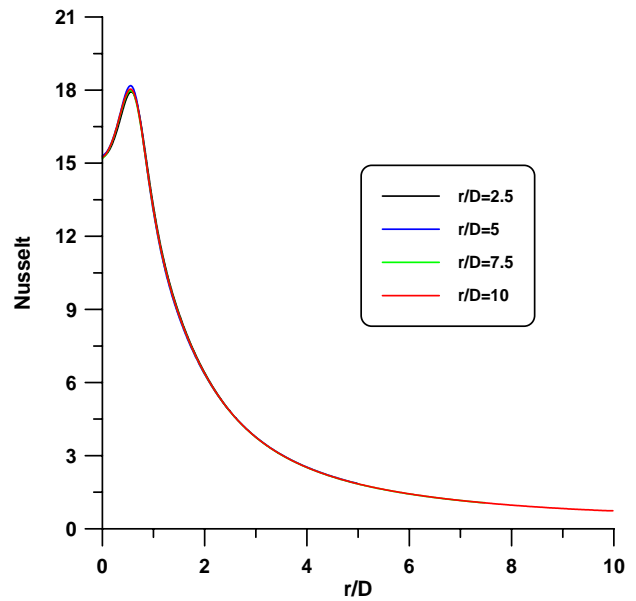


Figure 14. Local Nusselt number in the impingement surface for Re=500.

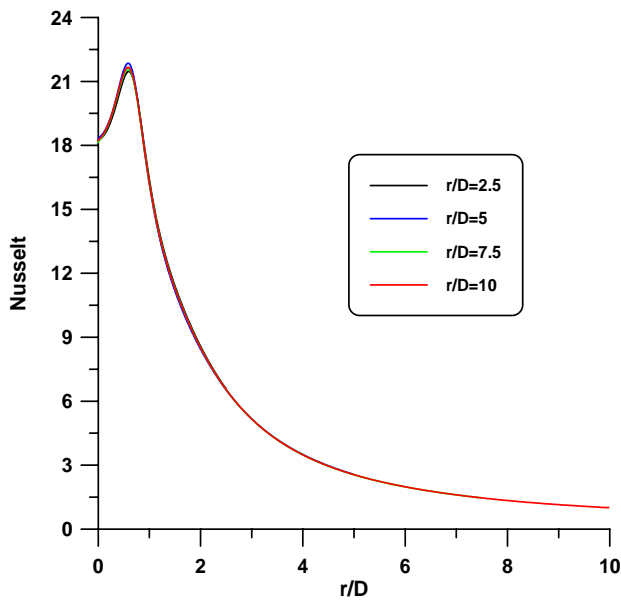


Figure 15. Local Nusselt number in the impingement surface for Re=750.

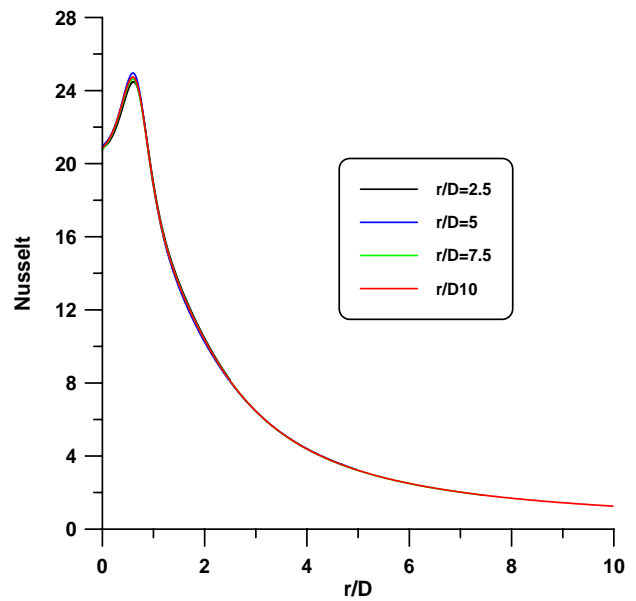


Figure 16. Local Nusselt number in the impingement surface for Re=1000.

The local Nusselt number increases with Reynolds number for all radial distance. The uniform inlet jet velocity produces a Nusselt number maximum away from the stagnation point, except for Reynolds number equal to 100, where the pick Nusselt number occurs at the jet center. It is observed that the difference between Nusselt number maximum and stagnation Nusselt number increases with Reynolds number.

Figure 17 shows the average Nusselt number determined as:

$$Nu_{av} = \frac{1}{A} \int_A Nu \, dA \quad \text{where } A - \text{impingement surface area} \tag{7}$$

As expected, the average Nusselt number ever increases with Reynolds number and decreases with r/D , because the local Nusselt number decreases abruptly when the radial distance increases.

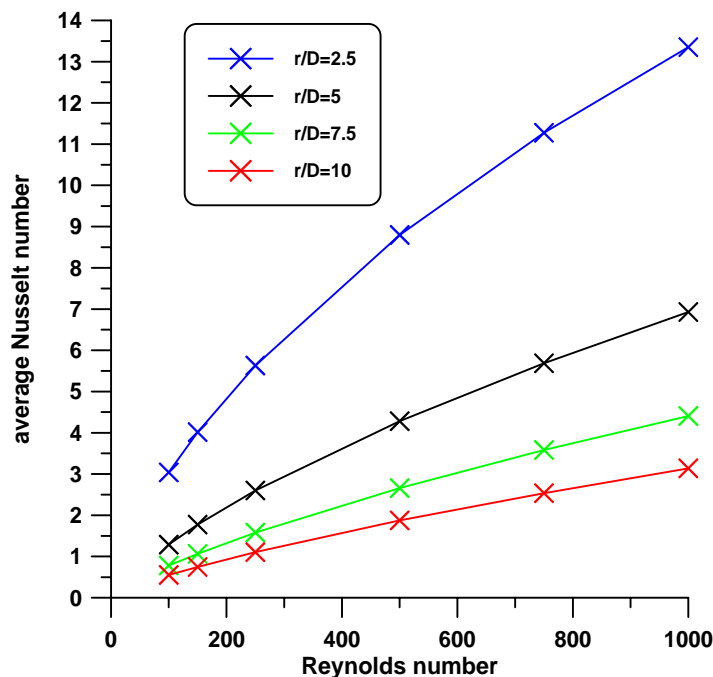


Figure 17. Average Nusselt number as a function of the Reynolds number.

Results presented in Fig. 17 can be extended to aid in predicting of an anti-icing thermal system based on an array of impingement hot air jets. During the design, it must be taken account that there is a better distance between the holes where: (i) one jet doesn't affect the performance of each other and (ii) energy loss doesn't occur.

6. FINAL COMMENTS

At the present work, the impingement jet problem on a flat surface was numerically simulated employing a CFD tool. Numerical results presented a good agreement with the experimental data. Besides, the Reynolds number effect and the domain extension were studied and showed that when the radial distance increases (r/D) results in a reduction of the average Nusselt number.

7. ACKNOWLEDGMENTS

The authors would like to acknowledge the *Empresa Brasileira de Aeronáutica – EMBRAER*, *Fundação de Amparo a Pesquisa do Estado de São Paulo – PICTA-FAPESP* (proc. 00/13768-4) and *Financiadora de Estudos e Projetos – FINEP-CAPTAER* (proc. N° 01-04-0663-00).

8. REFERENCES

- Baughn, J. W. and Shimizu, S., 1989, Heat transfer measurements from a surface with uniform heat flux and an impinging jet, *Journal of Heat Transfer, Transactions of the ASME*, v. 111, pp. 1096-1098.
- Baughn, J. W., Hechanova, A. E. and Yan, X., 1991, An experimental study of entrainment effects on the heat transfer from a flat surface to a heated circular impinging jet, *Journal of Heat Transfer*, v. 113, pp. 1023-1025.
- Behnia, M., Parneix, S and Durbin, P. A., 1998, Prediction of heat transfer in an axisymmetric turbulent jet impinging on a flat plate, *International Journal Heat and Mass Transfer*, v. 41, n. 12, pp. 1845-1855.
- Behnia, M., Parneix, S. and Durbin, P., 1997, Accurate modeling of impinging jet transfer, *Center for Turbulence Research, Annual Research Briefs*, pp. 149-164.
- Brown, J. M., Raghunathan, S., Watterson, J. K., Linton, A. J. and Riordon, D., 2002, Heat transfer correlation for anti-icing systems, *Journal of Aircraft*, v. 39, n. 1, pp. 65-70.
- Chattopadhyay, H., 2004, Numerical investigations of heat transfer from impinging annular jet, *International Journal of Heat and Mass Transfer*, v. 47, pp. 3197-3201.
- Coussirat, M., Beeck, J. van, Mestres, M., Egusguiza, E., Buchlin, J. M. and Escaler, X., 2005, Computational Fluid Dynamics modeling of impinging gas jet systems: I. Assessment of eddy viscosity models, *Journal of Fluid Engineering, Transactions of ASME*, v. 127, pp. 691-703.
- Fletcher, C. A. J., 1998, *Computational techniques for fluid dynamics, Fundamental and General Techniques*, Spring-

Verlag, Berlin, v. 1.

FLUENTTM Inc., 2006, User's guide, Version 6.2.16.

Saeed, F., Morency, F. and Paraschivoiu, I., 2000, Numerical Simulation of a hot-air anti-icing system, 38th Aerospace Sciences Meeting & Exhibit, AIAA 2000-0630, pp. 1-8.

Wright, W. B., 2004, An evaluation of jet impingement heat transfer correlations for piccolo tube application, NASA 2004-212917, AIAA 2004-0062, pp. 1-16.

9. RESPONSIBILITY NOTICE

The authors are the only responsible for the printed material included in this paper.